SUPPORTING INFORMATION

Supramolecular Assembly of Multicomponent Photoactive Systems *via* Cooperatively Coupled Equilibria

Miguel García-Iglesias,[a] *Katrin Peuntinger,*[b] *Jan Krausmann,*[b] *Axel Kahnt,*[b] *Purificación Vázquez,*[a] *David González-Rodríguez*[a], Dirk M. Guldi*[b] and Tomás Torres*[a,c]*

[a] Universidad Autónoma de Madrid, Departamento de Química Orgánica (C-I), Facultad de Ciencias, Cantoblanco, 28049-Madrid, Spain.

[b] Department of Chemistry and Pharmacy and Interdisciplinary Center for Molecular Materials (ICMM). Friedrich-Alexander-Universität Erlangen-Nürnberg. Egerlandstrasse 3, 91058 Erlangen, Germany.

[c] IMDEA-Nanociencia, c/ Faraday, 9, Campus de Cantoblanco, 28049 Madrid, Spain

SUPPORTING INFORMATION

Supporting Information Available:

SYNTHESIS AND CHARACTERIZATION

General Methods.

Synthesis and Characterization. Chemicals were purchased from commercial suppliers and used without further purification. Dry solvents were purchased from SDS in anhydrous grade and dried in addition, over molecular sieves (4Å size) acquired from SDS, as well. Prior to use the molecular sieves were dried in an oven during one night and subsequently activated by microwave oven-assisted irradiations took it in turns with a vacuum pump system. Column chromatography was carried out on silica gel Merck-60 (230-400 mesh, 60 Å). The monitoring of the reactions was carried out by TLC, employing aluminum sheets coated with silica gel 60 F254 (normal phase) or with LiChroprep RP-18 F254-S (reverse phase), both purchased from Merk. Purification of compounds was performed by flash column chromatography using silica gel Merck-60 (230-400 mesh, 0.040-0.063 mm) or Merck LiChroprep RP-18 F254-S (25-40 μm) for reverse phase. Organic eluants were purchased from SDS in a synthesis grade, while water for reverse phase was used in a milli-Q grade.

UV/Vis spectra were recorded with a Jasco V-630 with Peltier temperature control and the logarithm of the molar absorption coefficient (ε) is indicated in brackets for each maximum. Fluoresecence spectra were recorded with a Jasco FP-8600 with Peltier temperature control. IR spectra were recorded on a Bruker Vector 22 spectrophotometer. HRMS spectra were determined on a VG AutoSpec apparatus and MALDI-TOF-MS spectra were obtained from a BRUKER ULTRAFLEX III instrument equipped with a nitrogen laser operating at 337 nm. Dithranol (1,8,9-anthracenetriol) was found to be the most convenient matrix for these measurements. ESI Q-TOF spectra were recorded with a QSTAR instrument. NMR spectra were recorded with a BRUKER AC-300 (300 MHz) or a Bruker DRX-500 (500 MHz) instrument. The temperature was actively controlled at 298 K. Chemical shifts are measured in ppm relative to tetramethylsilane (TMS).

The synthetic route to **Pc1**, **C_{60}A** and **PTZP** is shown below in Schemes S1-S3. The synthesis and characterization of compounds **1**,[i] **C_{60}A**[ii] and **PTZP**[iii] has been described before. The synthesis and characterization of compounds **Pc1** and **2** is described below.

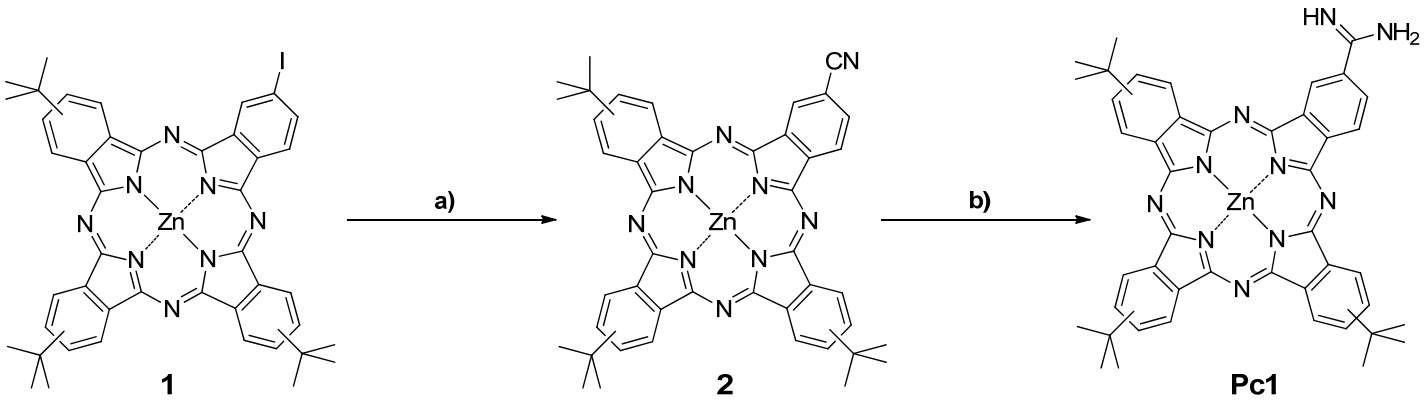

Scheme S1. Synthetic route to **Pc1**: a) $Pd(PPh_3)_4$, CuI, NaCN, PPh_3, THF, 65°C, 3h, 83%.[iv] b) $AlMe_3$, NH_4Cl, toluene, 80°C, 48h, 56%.[v]

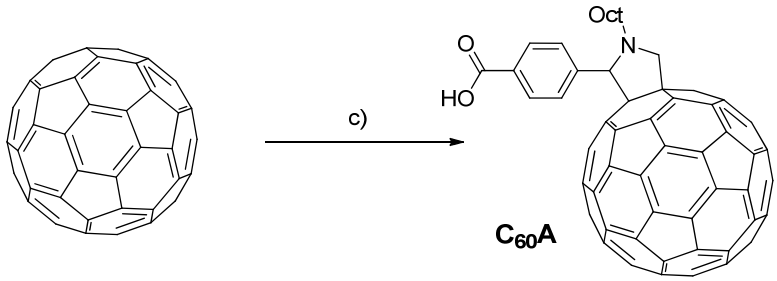

Scheme S2. Synthetic route to **C_{60}A**:[ii] c) N-Octylglycine, 4-formylbenzoic acid, oDCB, reflux, 16h, 51%.

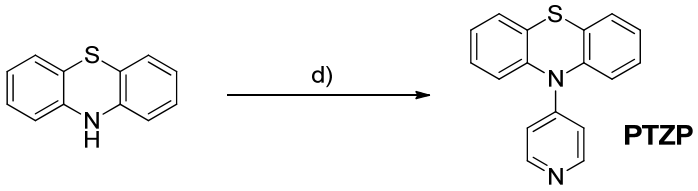

Scheme S3. Synthetic route to **PTZP**:[iii] d) 4-bromopyridine hydrochloride, $Pd(OAc)_2$, BINAP, t-BuOK, toluene, 70°C, 16h, 57%.

9(10),16(17),23(24)-Tri-*tert*-butyl-2-cyano-5,28:14,19-diimino-7,12:21,26-dinitrilo-tetrabenzo[c,h,m,r][1,6,11,16]tetraazacicloeicosinato-(2)-N^{29},N^{30},N^{31},N^{32}zinc(II) (mixture of regioisomers) (2)

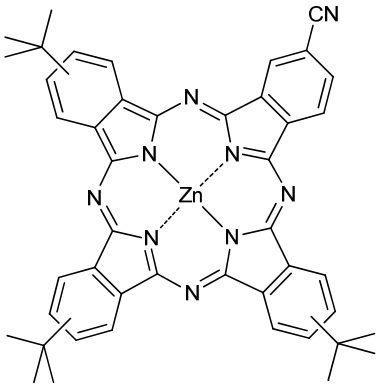

A mixture of iodophthalocyanine **1**[i] (50 mg, 0.057 mmol), CuI (1.1 mg, 0.057 mmol), NaCN (5.6 mg, 0.114 mmol), $Pd(PPh_3)_4$ (3.3 mg, 0.0028 mmol) and PPh_3 (1.5 mg, 0.0057 mmol) in 3.0 mL of dry THF was heated at 65 ºC in argon atmosphere for 3h. After evaporation of the solvent the crude was finally purified by column chromatography [(SiO_2), hexane/dioxane (4:1)]. The solid obtained was triturated in methanol (2x20 mL) and hexane (2x20 mL), filtered and dried, yielding 36.4 mg (83%) of **2** as a dark green solid.

M.p.: > 250 ºC. **^{1}H NMR** (500 MHz, [d_6]DMSO, 25 ºC, TMS), δ = 9.5-8.6 (m, 8H; PcH), 8.5-8.2 (m, 3H, PcH, PcHCN), 7.7-7.5 (m, 2H, PcHCN), 1.9-1.7 (s, 27H; $C(CH_3)_3$) ppm. **FT-IR** (KBr): 3495, 2962, 2222 (C≡N), 1616, 1483, 1389, 1335, 1254, 1178, 1084, 1070, 972, 833, 744, 690 cm^{-1}. **UV/Vis** (THF): λ_{max} (log ε) = 687 (5.2), 664 (5.1), 631 (4.4), 601 (4.4), 346 (4.8) nm. MS (MALDI-TOF, dithranol: m/z (%) 769.3-777.3 (100) $[M]^+$. **HR MALDI-TOF MS**, dithranol: *m/z* 769.26144 [M^+], calcd for $C_{45}H_{39}N_9Zn$: 769.26147.

^{1}H NMR of 2

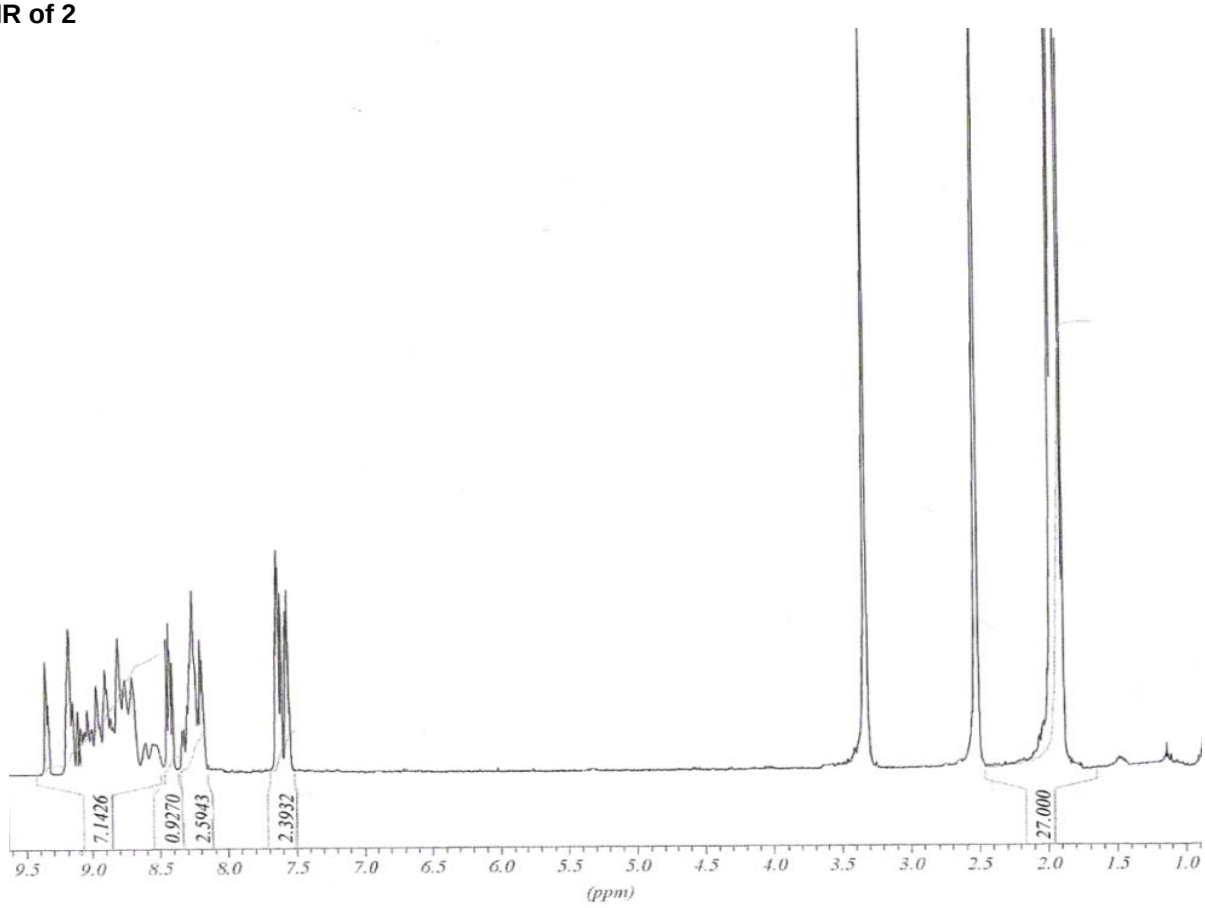

UV-vis of 2

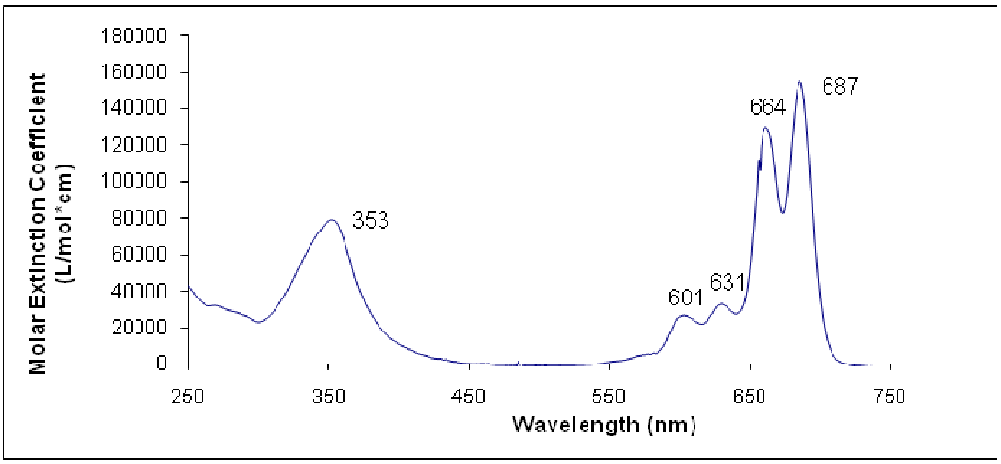

MALDI-TOF spectra with (inset) isotopic distribution pattern (a), and HR-MALDI-TOF spectrum (b) of 2

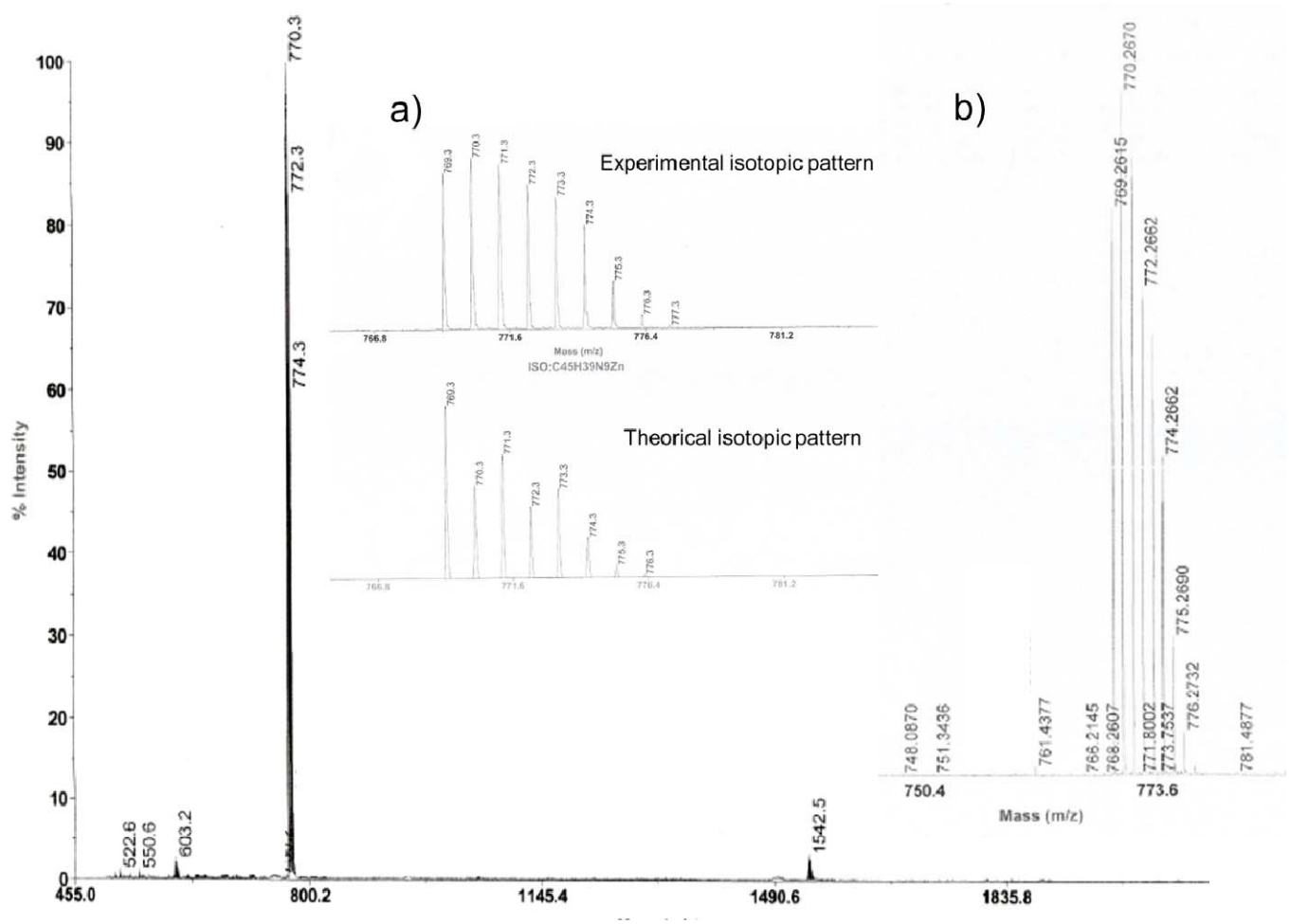

FT-IR spectra of 2

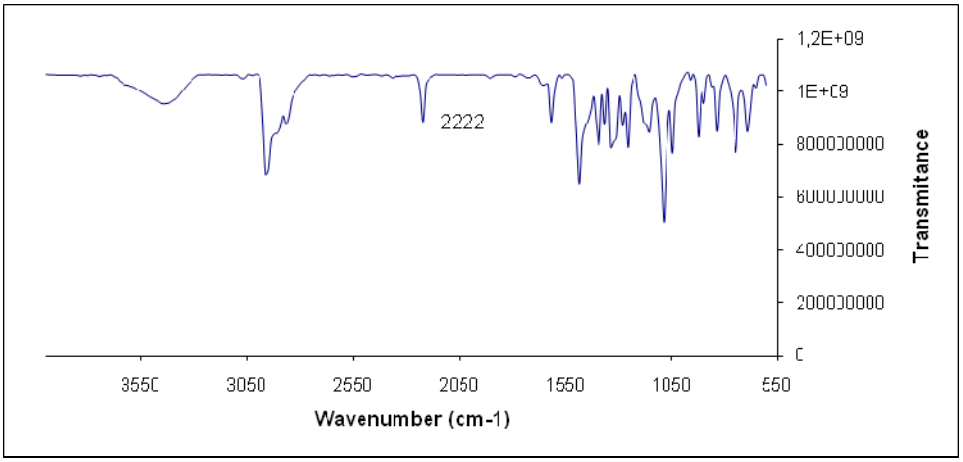

9(10),16(17),23(24)-Tri-*tert*-butyl-2-carbamidinoyl-5,28:14,19-diimino-7,12:21,26-dinitrilo-tetrabenzo[c,h,m,r][1,6,11,16]tetraazacicloeicosinato-(2)-N^{29},N^{30},N^{31},N^{32}zinc(II) (mixture of regioisomers) (Pc1)

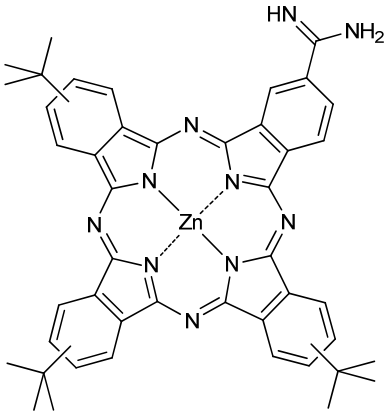

A solution of $AlMe_3$ in hexanes (2m, 0.80 mL) was added to a suspension of **2** (123 mg, 0.16 mmol) and NH_4Cl (86 mg, 1.6 mmol) in dry toluene (10 mL). The mixture was stirred at 80°C for 48 h under Ar in the dark. The reaction mixture was poured into 50 mL of H_2O and extracted with AcOEt (2 x 40 ml). The organic layer was separated, washed with a saturated aqueous solution of $NaHCO_3$ (2x60 mL), brine (2x60 mL) and dried over Na_2SO_4. After filtration of the drying agent, the solvent was evaporated and the green solid was purified on a chromatographic column (reverse phase, THF/water (3:1)). The solution was washed with brine (2x60 mL) and the solvent was removed obtaining **Pc1** (70 mg, 56%) as a green solid.

M.p.: > 250 ºC. **^{1}H NMR** (500 MHz, [d_6]DMSO, 25 ºC, TMS), δ = 9.8-9.0 (m broad, 8H; PcH), 8.8-8.2 (m broad, 4H, PcH), 7.0-5.4 (m broad, 2H, amidine)1.9-1.7 (s, 27H; C(CH3)3) ppm. **FT-IR** (KBr): 3470, 2902, 1641 (C=N), 1997, 1389, 1331, 1281, 1157, 1090, 1076, 926, 837, 798 cm^{-1}. **UV/Vis** (THF): λ_{max} (log ε) = 694 (5.2), 669 (5.1), 617 (4.5), 348 (4.8) nm. MS (MALDI-TOF, dithranol: m/z (%) 786.3-793.3 (100) $[M]^+$. **HR MALDI-TOF MS**, dithranol: *m/z* 786.28799 [M^+], calcd for $C_{45}H_{42}N_{10}Zn$: 786.28857.

^{1}H NMR of Pc1

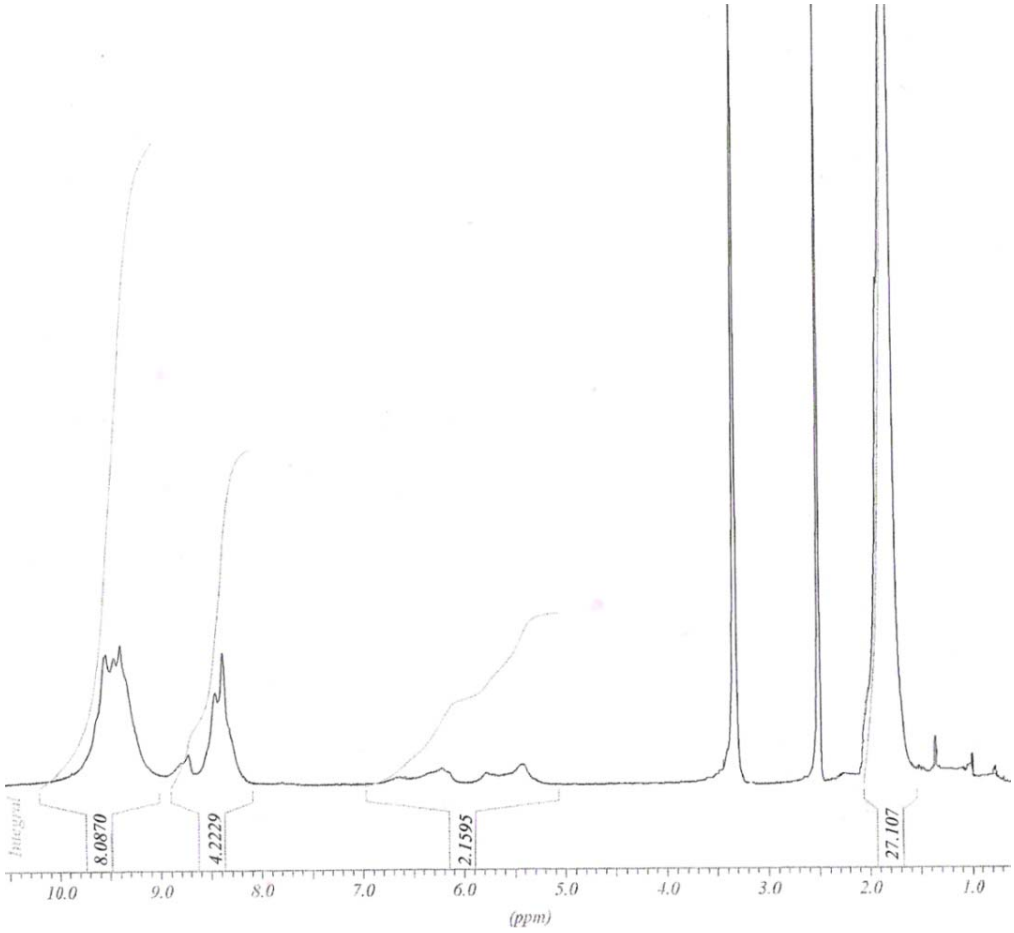

UV-vis of Pc1

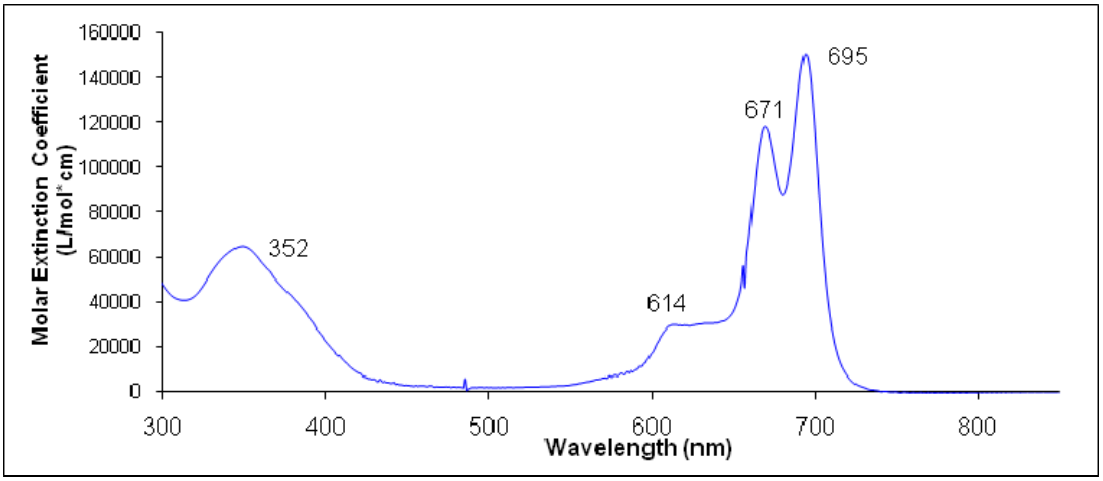

MALDI-TOF spectra with (inset) isotopic distribution pattern (a), and HR-MALDI-TOF spectrum (b) of Pc1

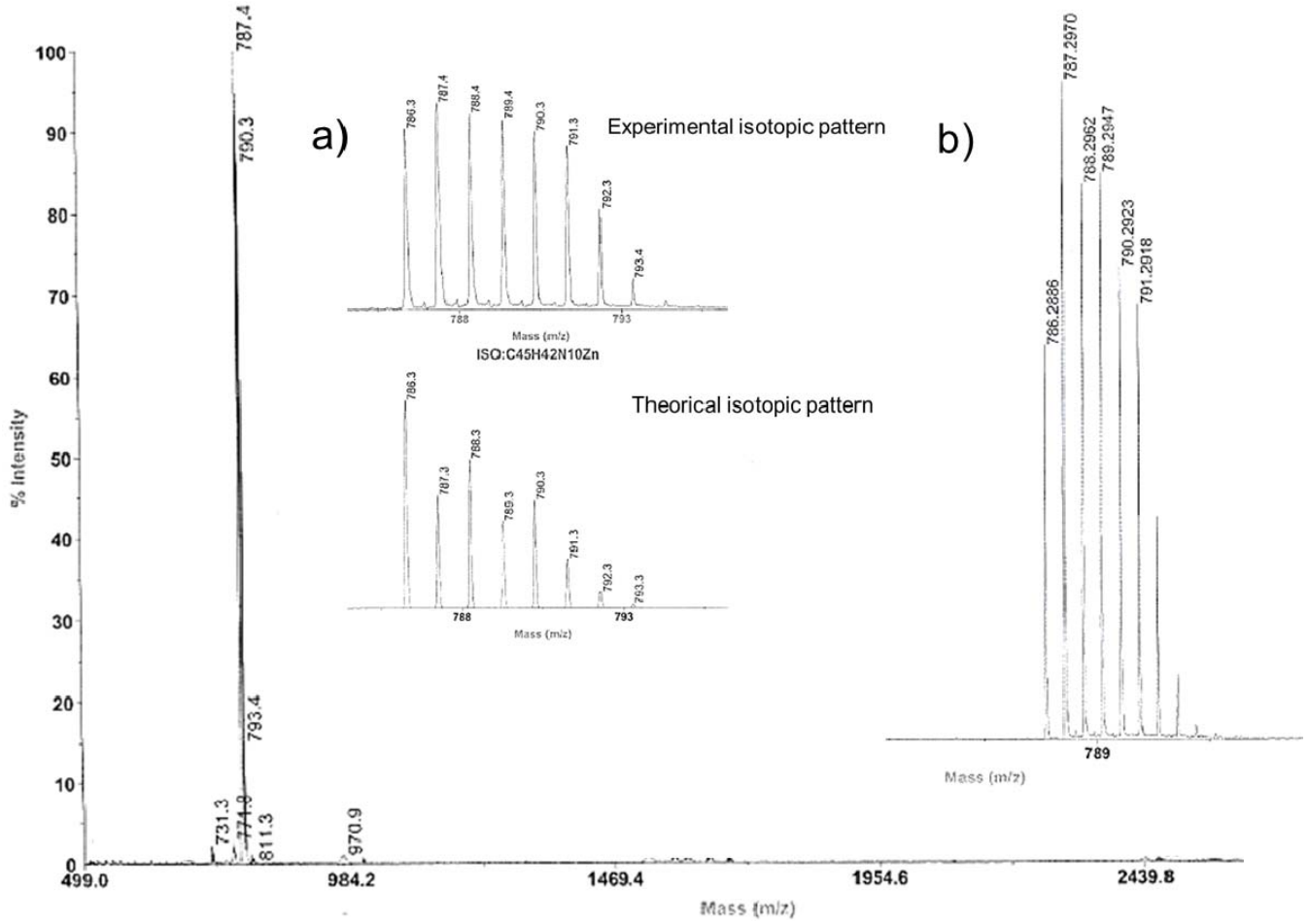

FT-IR spectra of Pc1

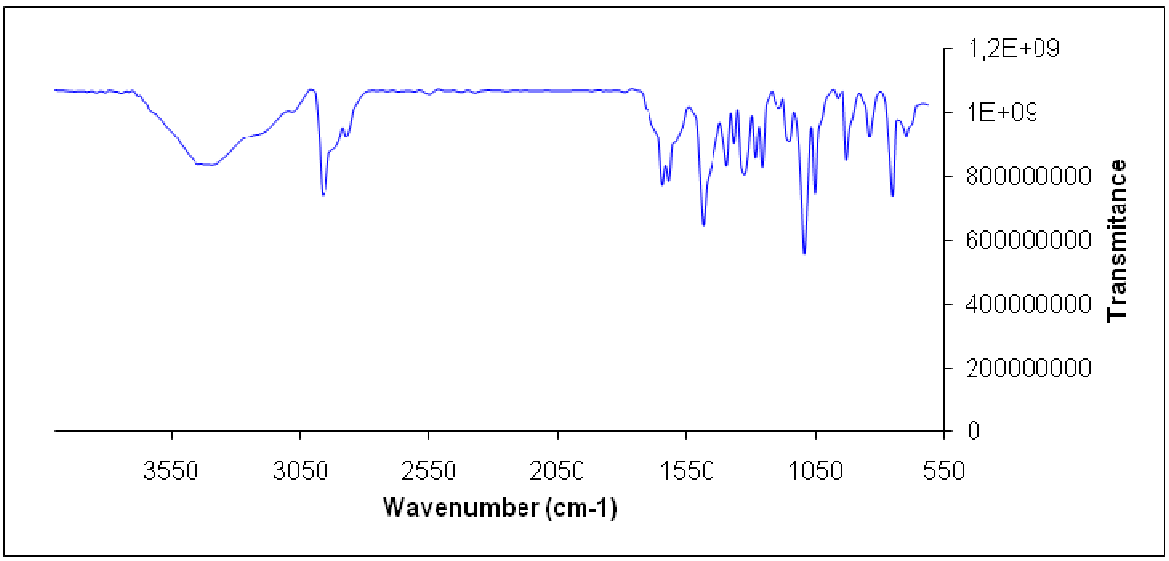

ADDITIONAL SUPPORTING INFORMATION

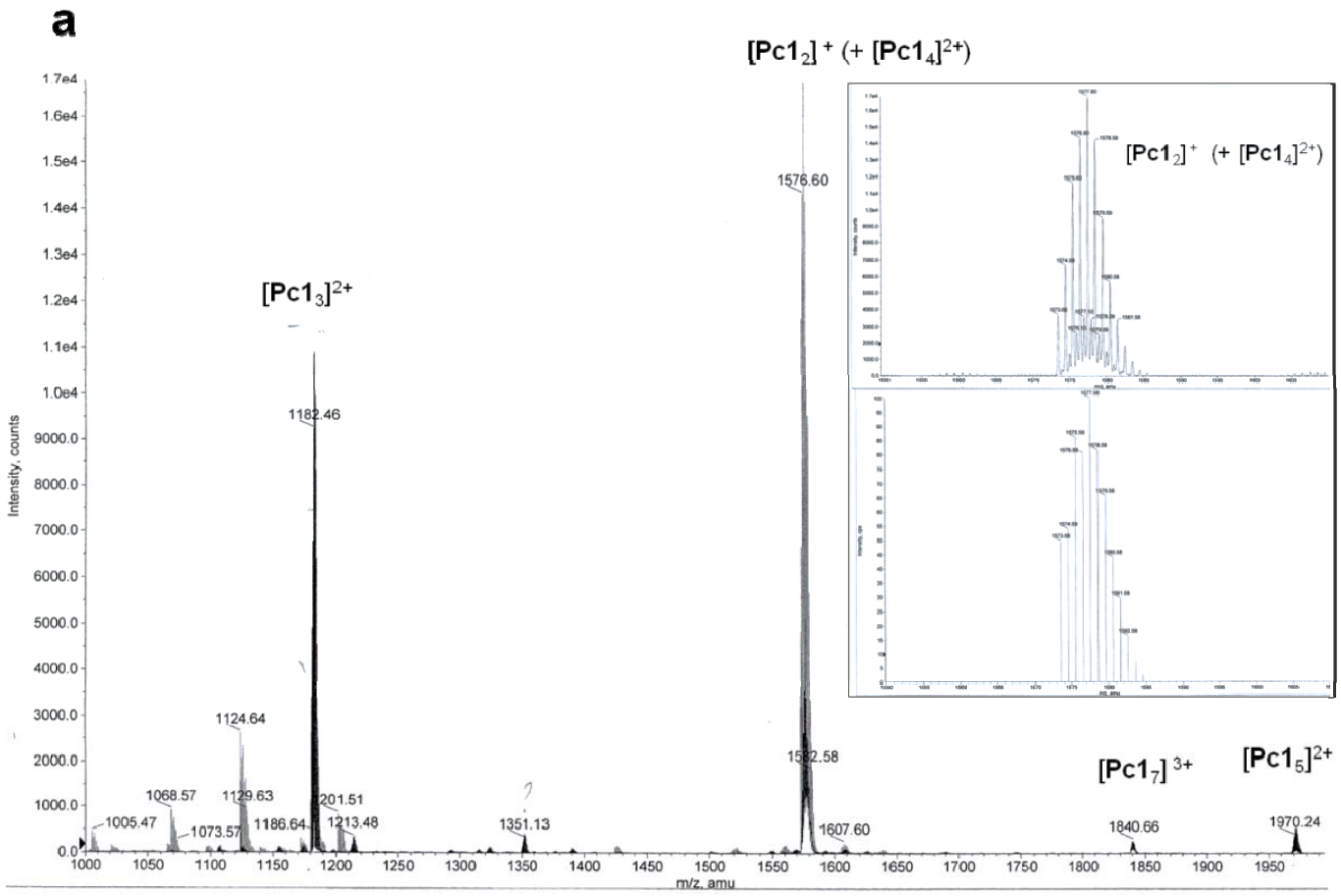

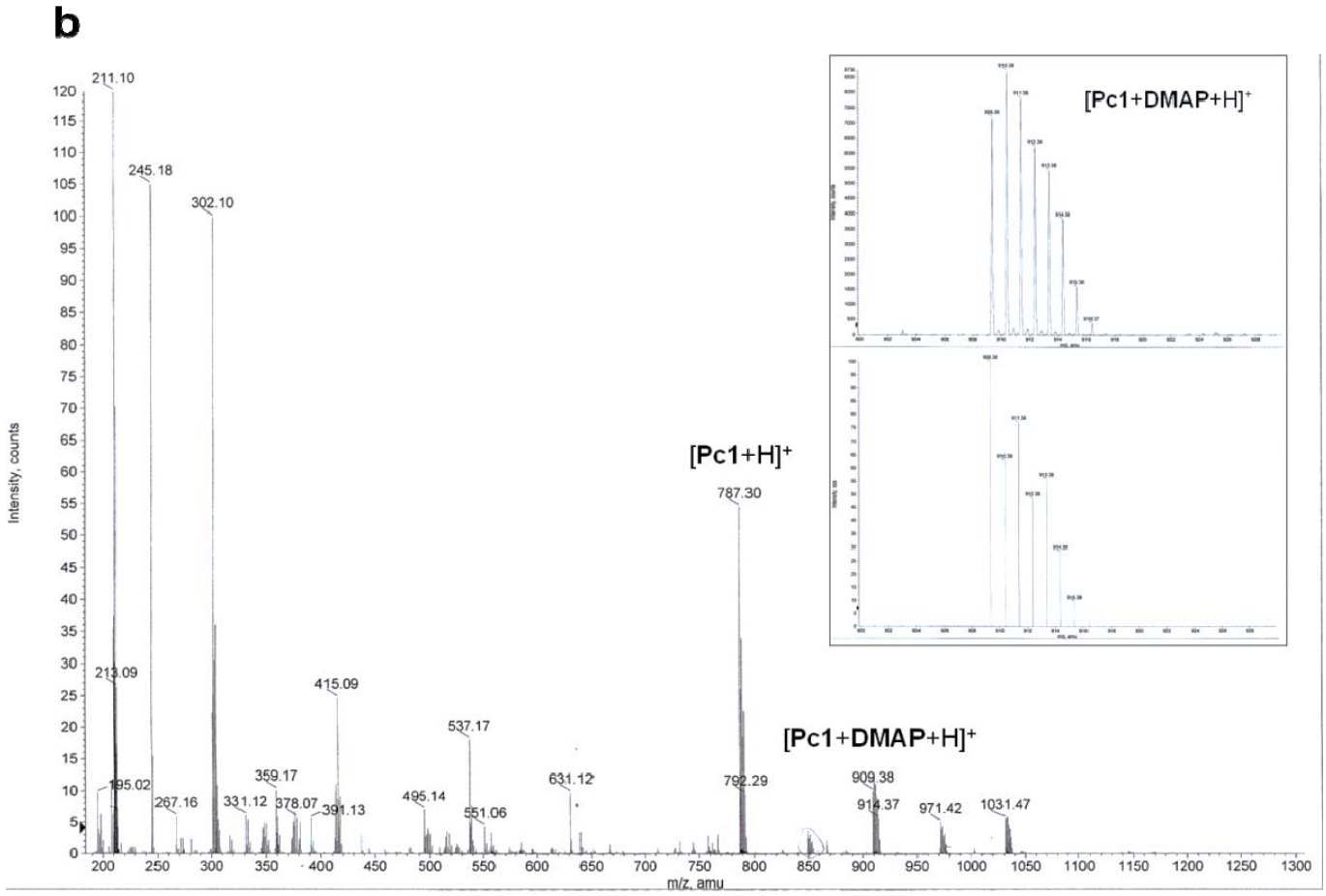

FIGURE S1. (**a**) Portion of the ESI Q-TOF mass spectra of **Pc1** showing the detection of charged oligomers in the gas phase. Inset: Experimental (top) and theoretical (bottom) isotopic distribution of the $[\mathbf{Pc1}_2]^+$ ion. A small amount of the $[\mathbf{Pc1}_4]^{2+}$ ion is also present in the same region.(**b**) ESI Q-TOF mass spectra of **Pc1** in the presence of 5 eqs. **DMAP** and 5 eqs. **EBA** showing the suppression of oligomeric species and the detection of the charged $[\mathbf{Pc1}+\mathbf{DMAP}+H]^+$ complex. Inset: Experimental (top) and theoretical (bottom) isotopic distribution of the $[\mathbf{Pc1}+\mathbf{DMAP}+H]^+$ ion. In both cases: positive mode; ionizing phase: MeOH.

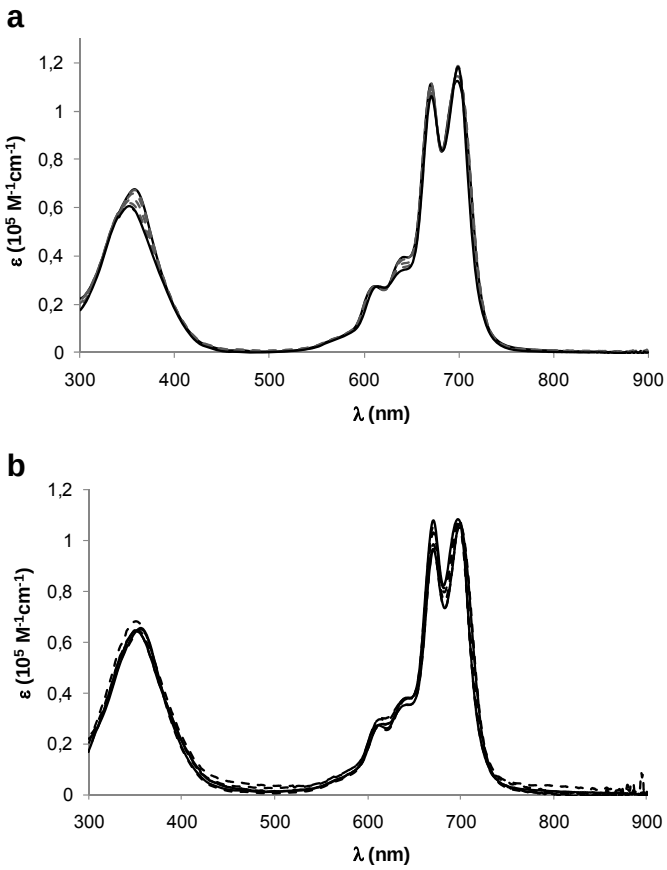

FIGURE S2. Changes in the absorption spectra of **Pc1** in toluene as a function of (**a**) temperature (from 20ºC to 90ºC; [**Pc1**] = 8.0 x 10^{-6} M) and (**b**) concentration (from 1.6 x 10^{-4} M to 8 x 10^{-8} M; T = 20ºC). These experiments demonstrate the high stability of (**Pc1**)$_2$ to concentration or temperature changes

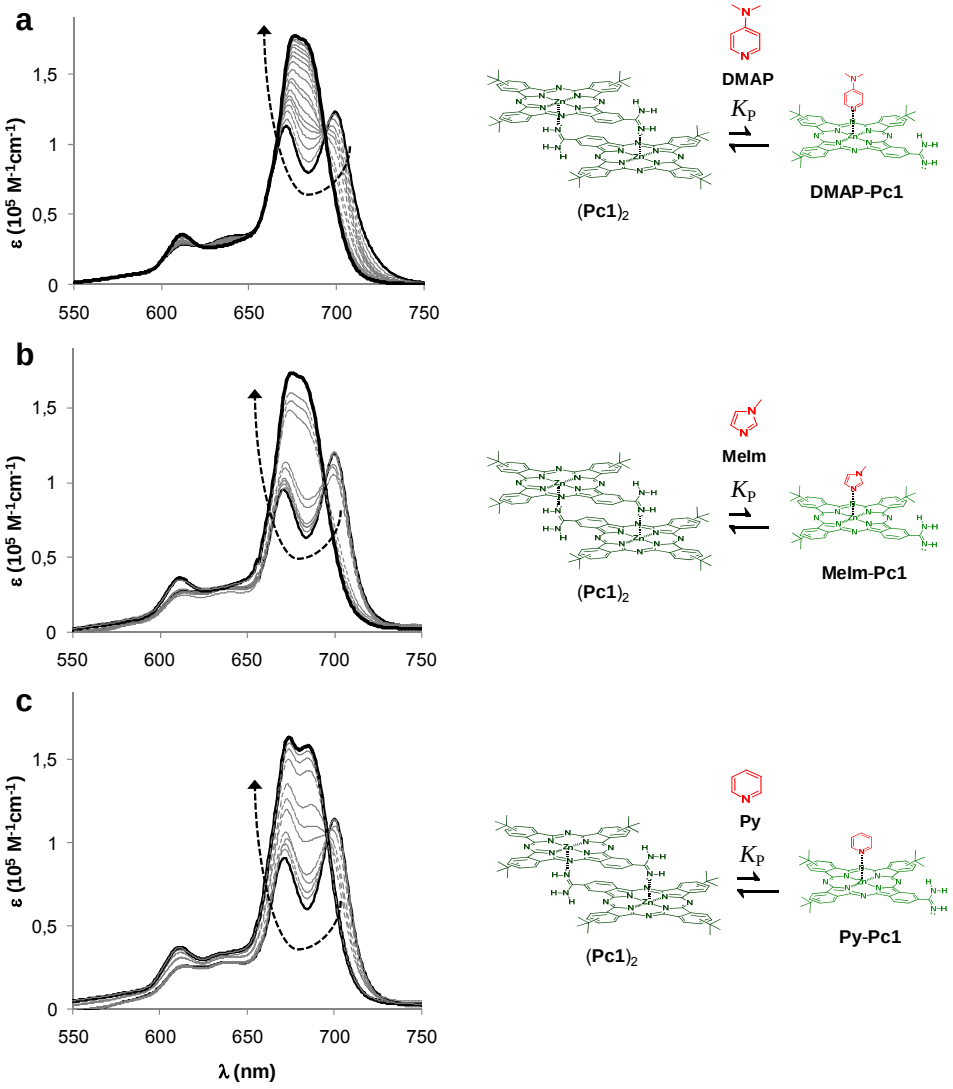

FIGURE S3. Spectral changes attributed to the dissociation of (**Pc1**)$_2$ by competition with Zn-coordinating ligands (P) to yield P-**Pc1**. Please note the high similarity of the absorption changes in each case and also when compared to related Pc-imidazole cofacial dimers described by Kobuke et al. (ref. 7 in the manuscript). Changes in the absorption spectra of (**Pc1**)$_2$ ([**Pc1**] = 8 x 10^{-6} M) in toluene with the addition of increasing amounts of (**a**) dimethylaminopyridine (**DMAP**) (up to 2 x 10^4 eqs), (**b**) N-methylimidazole (**MeIm**) (up to 2 x 10^4 eqs), or (**c**) pyridine (**Py**) (up to 10^5 eqs.), showing the dissociation of (**Pc1**)$_2$.

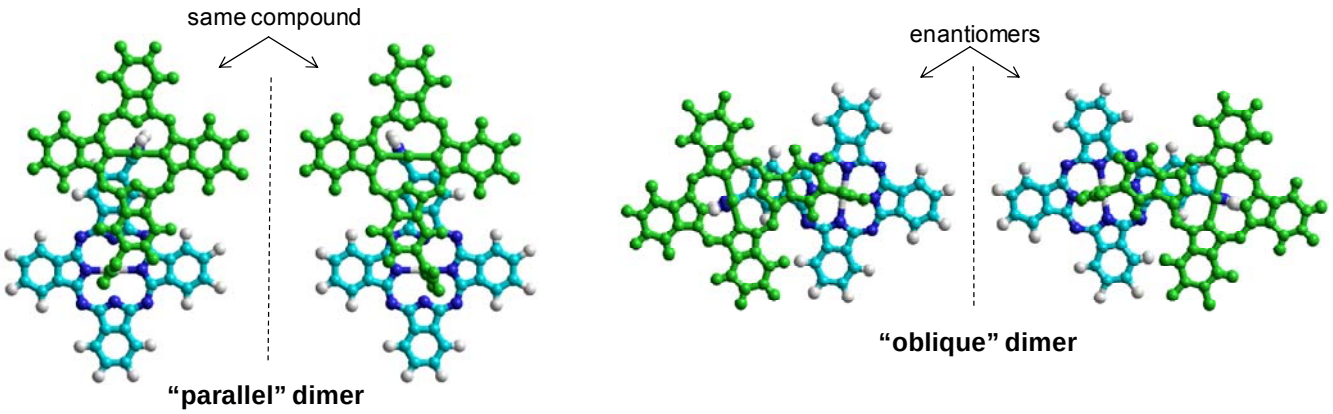

FIGURE S4. Models of the dimer isomers formed from **Pc1**: “parallel”+ 2 “oblique” enantiomers. The *tert*-butyl groups have been omitted for clarity. The Pc in green is on top.

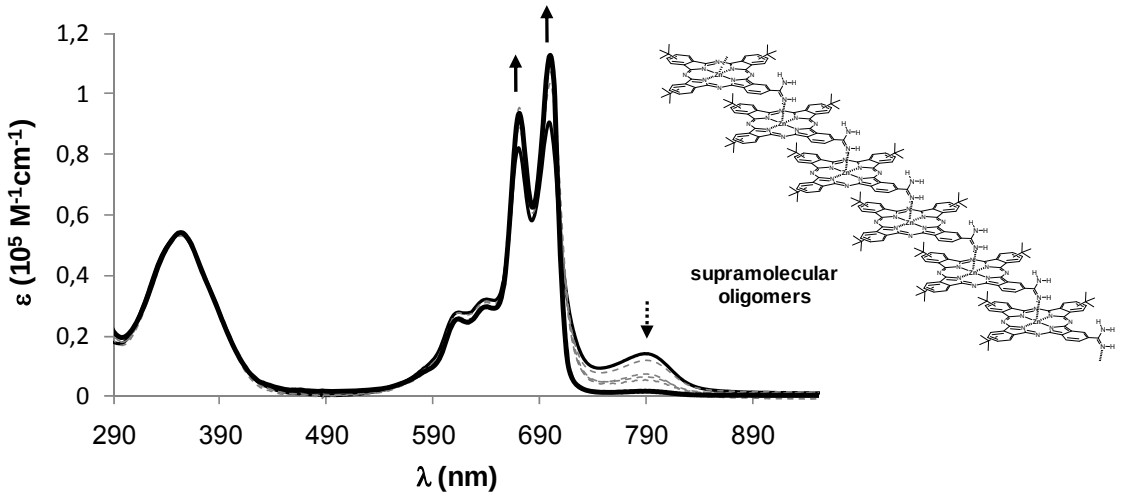

FIGURE S5. Absorption spectra of **Pc1** in toluene ([**Pc1**] = 8.0 x 10^{-6} M) as a function of time (from 1 to 10 hours), showing the disappearance of the band at 788 nm. The sample was prepared by fast and thorough drying (100 ºC, overnight) of a solution of **Pc1** in dry toluene ([**Pc1**] = 8 x 10^{-5} M), and then measuring absorption just after total redissolution (addition of 10 mL of dry toluene). The same changes were observed within 1 hour at 60ºC. Structure of a hypothetic supramolecular oligomer obtained from **Pc1** upon concentration to the solid state that slowly interconverts to the thermodynamically stable dimer in diluted samples.

Determination of the dimerization constant (K_D) of Pc1 through competition experiments

In order to evaluate the high dimerization constant of **Pc1** we used an indirect method previously employed by the group of Kobuke.[vi] When, A, ε, M, and D represent absorbance, molar absorption coefficient, **Pc1**, and dimer (**Pc1**)$_2$, respectively, the following equations hold.

$$A = A_M + A_D = \varepsilon_M \cdot [M] + \varepsilon_D \cdot [D] \qquad \text{(Eq. 1)}$$

$$[D] = [D]_0 - 1/2[M] = [D]_0 - A_M/2\varepsilon_M \qquad \text{(Eq. 2)}$$

Since the initial solution is considered to contain dimer only, we assume Eq. 3.

$$A_0 = \varepsilon_D \cdot [D]_0 \qquad \text{(Eq. 3)}$$

These relations lead to Eq. 4:

$$A_M = (2\varepsilon_M \cdot (A - A_0)) / (2\varepsilon_M - \varepsilon_D) \qquad \text{(Eq. 4)}$$

The value of ε_M was evaluated from the absorption at the final titration point. The reaction equilibrium equation (Eq. 5) can be rewritten using Eq. 4 as Eq. 7, where [P] is the concentration of N-containing ligand (i.e. pyridine, DMAP, or N-methylimidazole) .

$$D + 2\,P \rightarrow 2\,M\text{-}P \qquad K_P = [M\text{-}P]^2 / [D]\cdot[P]^2 \qquad \text{(Eq. 5)}$$

$$K_P = [M]^2 / (([D]_0 - [M]/2)\cdot([P] - [M]^2)) \qquad \text{(Eq. 6)}$$

$$K_P = (A_M/2\varepsilon_M)^2 / (((A_0/\varepsilon_D) - (A_M/2\varepsilon_M))\cdot([P] - (A_M/2\varepsilon_M)^2)) \qquad \text{(Eq. 7)}$$

In the titration experiments with pyridine in toluene, A_M (calculated as Eq. 4) at 676 nm was plotted as a function of [P] at every titration point. The best nonlinear fit rendered K_P = 1.1 x 10^4 M^{-1}. A similar analysis was performed using the fluorescence titration data at 701 nm yielding K_P = 2.3 x 10^4 M^{-1}. Then, considering the different equilibria below and the relationship between their equilibrium constants, and assuming that the association constant of **Pc1** and pyridine (K_1) can be approximated by the association constant between tetra(*tert*-butyl)ZnPc and pyridine in toluene (K_1' = 6.1 x 10^3 M^{-1}),[vii] we derived the dimerization constant K_D.

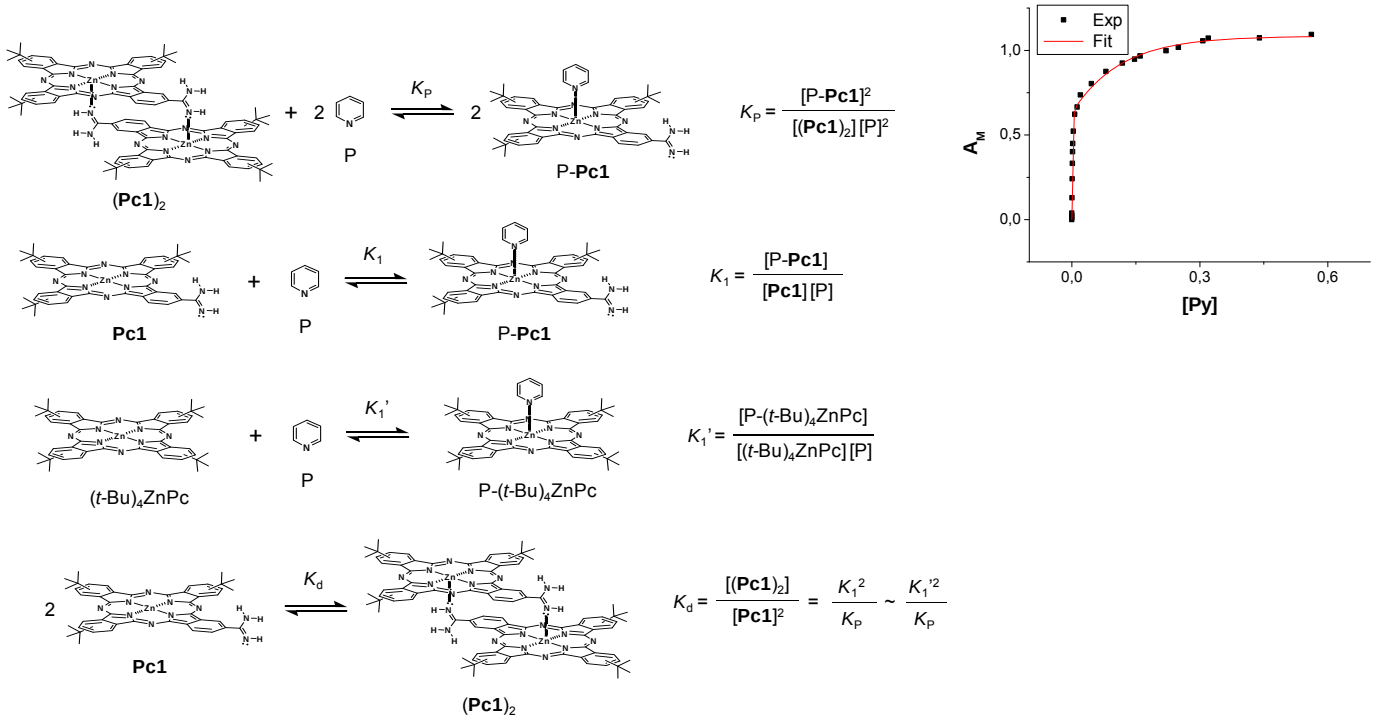

FIGURE S6. Different equilibrium reactions considered for the evaluation of the dimerization contant (K_D) of dimer (**Pc1**)$_2$ through competition titration experiments. Inset: fitting of the absorbance changes on titration of (**Pc1**)$_2$ with pyridine to determine K_P.

Estimation of the association constant (K_T) of dimer $(Pc1)_2$ with pyridine (P) and carboxylic acid (A) ligands

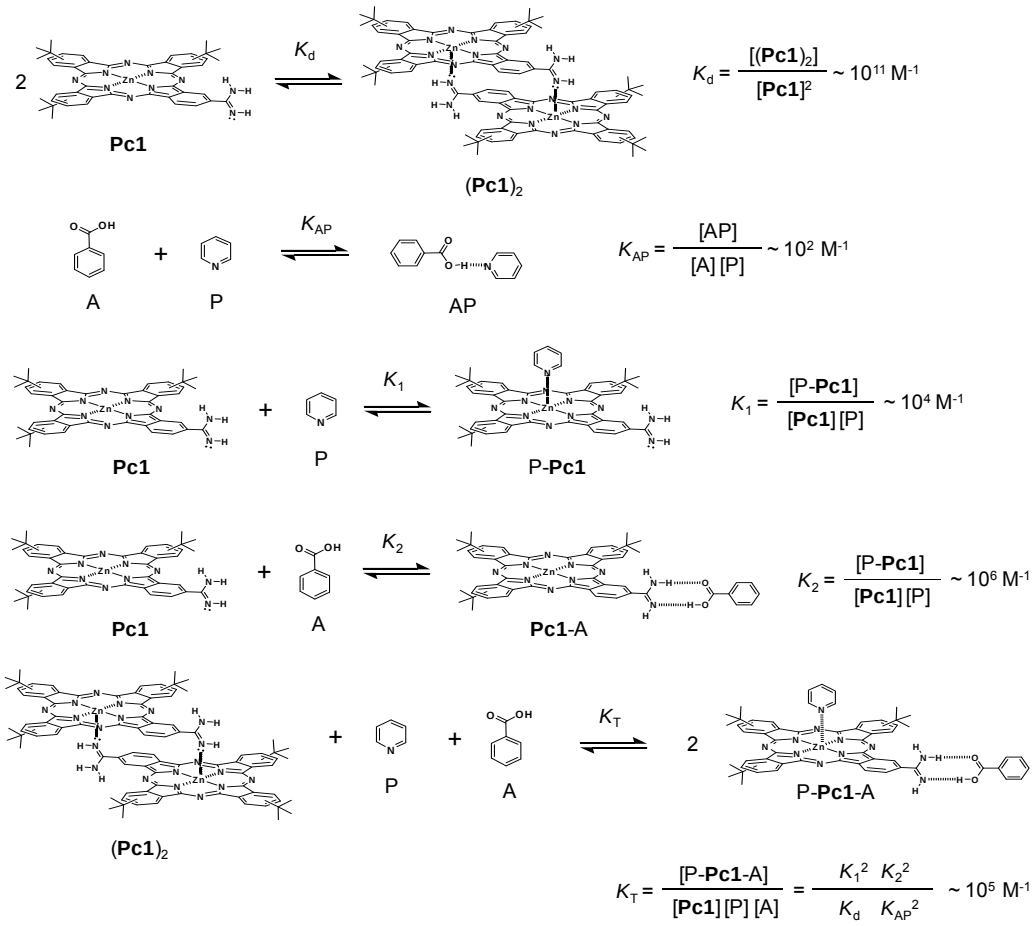

FIGURE S7. Different equilibrium reactions considered for the rough estimation of the association constant (K_T) of dimer (**Pc1**)$_2$ with pyridine (P) and carboxylic acid (A) ligands. The different association constants (K_{AP}, K_1, K_2) were taken from suitable reported values.

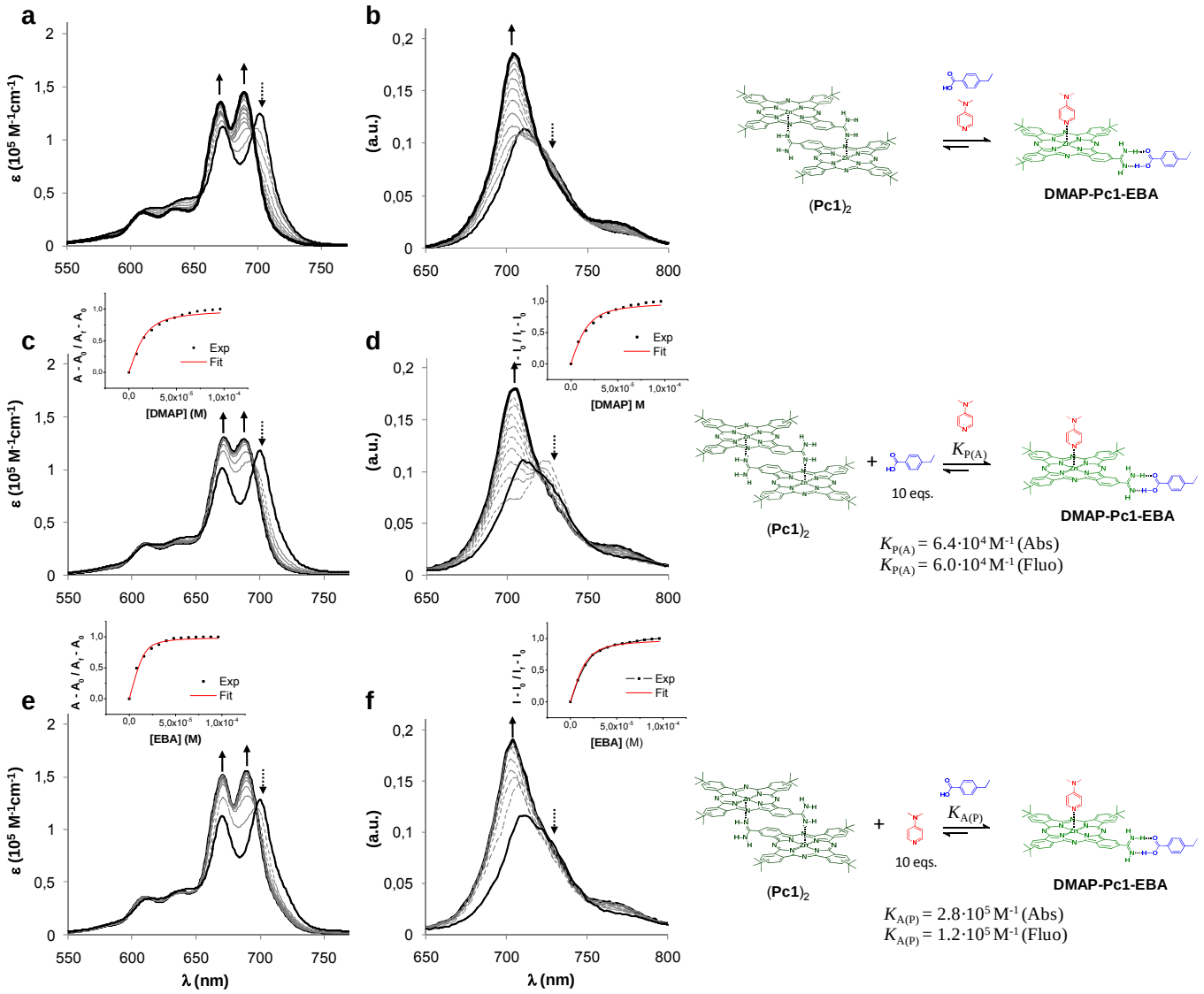

FIGURE S8. Titration experiments of (**Pc1**)$_2$ toluene solutions with **DMAP** and **EBA** varying the addition order. **Pc1** ([**Pc1**] = 8x10^{-6} M) *Q*-band absorption (**a**,**c**,**e**) and emission (**b**,**d**,**f**) changes that occur upon: (**a**,**b**) addition of a 1:1 mixture of **DMAP** and **EBA** up to 5 eqs. of each ligand, (**c**,**d**) addition of **DMAP** (up to 2 eqs.) in the presence of 10 eq. of **EBA** and, (**e**,**f**) addition of **EBA** (up to 2 eqs.) in the presence of 10 eq. of **DMAP**. In the emission spectra (**b**,**d**,**f**) samples were excited at 597 nm. The last two titration experiments (i.e. **c**, **d** and **e**, **f**) allowed us to evaluate the apparent binding constants of **DMAP** ($K_{P(A)}$) or **EBA** ($K_{A(P)}$) to **Pc1** solutions containing a 10-fold excess of the complementary ligand (**EBA** or **DMAP**, respectively). Insets in **c**,**d**,**e**,**f** show the fitting of the absorption (at 691 nm) or emission (at 704 nm) intensity changes with ligand (**DMAP** (**c**,**d**) or **EBA** (**e**,**f**)) concentration to determine $K_{P(A)}$ or $K_{A(P)}$, respectively. Please note that the same final absorption and emission stationary states (as those shown in Figures 1e and 1f) was reached by going through clear isosbestic points when choosing any other **DMAP** / **EBA** addition order, which underlines the cooperative nature of these equilibria.

PHOTOPHYSICS

General Methods.

Steady state UV-vis absorption. Steady-state UV-vis absorption spectroscopy was performed on a Lambda2 spectrometer (Perkin Elmer).

Steady state fluorescence. Steady state fluorescence spectra were carried out at a FluoroMax3 spectrometer (Horiba) in the visible detection range and at a FluoroLog3 spectrometer (Horiba) with a IGA Symphony (512x1x1 µm) detector in the NIR detection range.

Time Resolved Fluorescence Spectroscopy. Fluorescence lifetimes were determined by the time correlated single photon counting technique using a FlouroLog3 emission spectrometer (Horiba JobinYvon) equipped with an R3809U-58 MCP (Hamamatsu) and an N-647L laser diode (Horiba JobinYvon) exciting at 647 nm (≤200 ps fwhm).

Femtosecond Transient Absorption. Transient absorption (TA) experiments were carried out with an amplified Ti:Sapphire laser system CPA-2101 fs laser (Clark MXR: output 775 nm, 1 kHz, and 150 fs pulse width) using a transient absorption pump/probe detection system (TAPPS Helios, Ultrafast Systems). The 660 nm excitation wavelength was generated with a noncollinear optical parametric amplifier (NOPA, Clark MXR). For the, excitation wavelength the energy of 200 nJ/ pulse was selected.

Nanosecond transient absorption. Nanosecond transient absorption experiments were carried out with a Nd:YAG laser. The 532 nm excitation wavelength was formed by second harmonic generation. Moreover, pulse widths of less than 5 ns with energies of up to 7 mJ were selected. The optical detection was based on a pulsed Xenon lamp, a monochromator, a photomultiplier tube or a fast silicon photodiode with a 1 GHz amplification and a 500 MHz digital oscilloscope. The laser power of every laser pulse was registered using a bypath with a fast silicon photodiode. The experiments were performed in a 5x10 mm quartz glass cuvette.

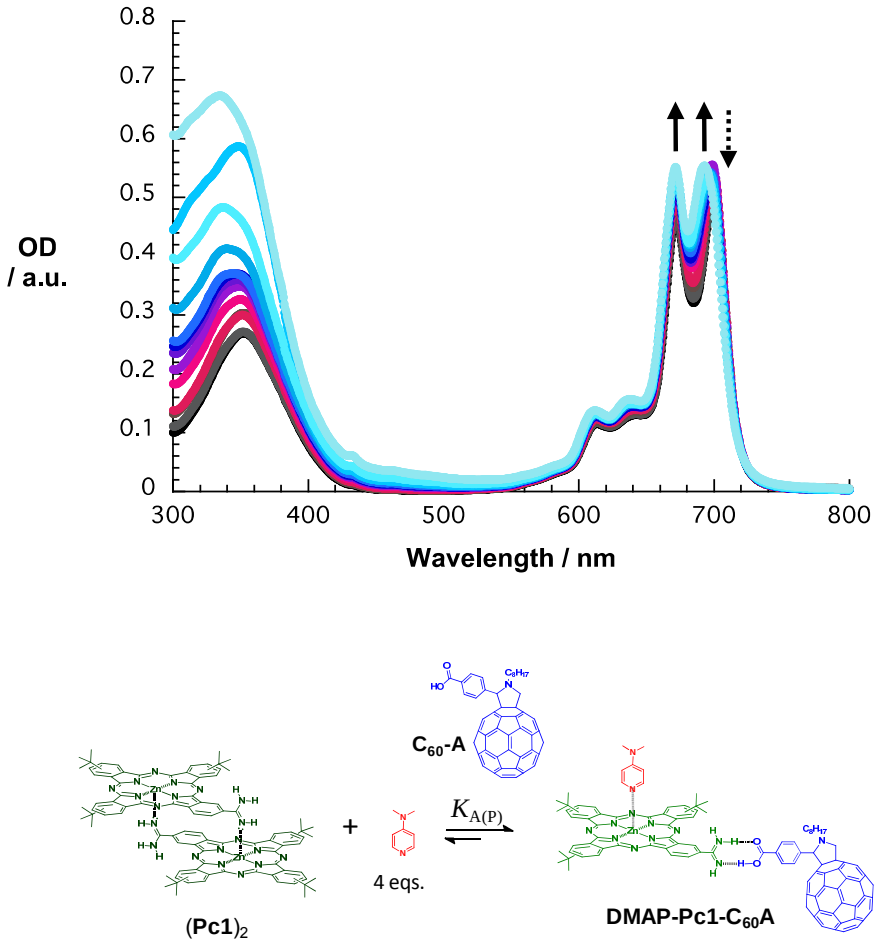

FIGURE S9. Absorption titration of **Pc1** (5.33 x 10^{-6} M) and **DMAP** (1.50 x 10^{-5} M) with an increasing addition of **C_{60}A** from 0 to a concentration of 4.5 x 10^{-5} M (from black over red to light blue – 0, 5.0 x 10^{-7}, 1.0 x 10^{-6}, 1.5 x 10^{-6}, 3.21 x 10^{-6}, 4.02 x 10^{-6}, 5.0 x 10^{-6}, 5.22 x 10^{-6}, 6.02 x 10^{-6}, 7.5 x 10^{-6}, 8.03 x 10^{-6}, 1.0 x 10^{-5}, 1.5 x 10^{-5} M) in toluene at room temperature. Please compare with Figures S8 and 1e.

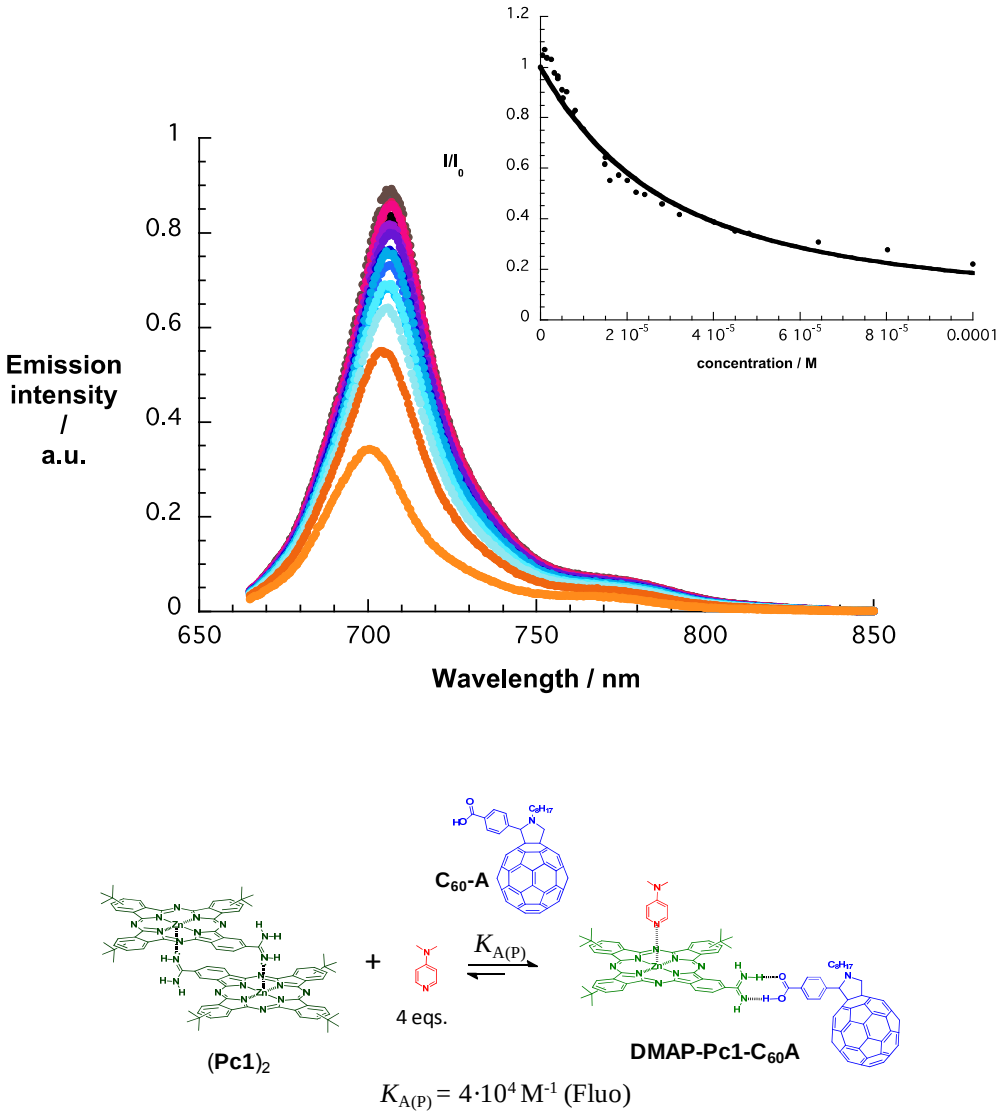

FIGURE S10. Emission titration of **Pc1** (5.33 x 10^{-6} M) and **DMAP** (1.50 x 10^{-5} M) with an increasing addition of **C_{60}A** from 0 to a concentration of 4.5 x 10^{-5} M (from black over red and light blue to orange – 0, 5.0 x 10^{-7}, 1.0 x 10^{-6}, 1.5 x 10^{-6}, 2.5 x 10^{-6}, 3.21 x 10^{-6}, 4.02 x 10^{-6}, 5.0 x 10^{-6}, 5.22 x 10^{-6}, 6.02 x 10^{-6}, 7.5 x 10^{-6}, 8.03 x 10^{-6}, 1.0 x 10^{-5}, 1.5 x 10^{-5}, 4.5 x 10^{-5} M) in toluene at room temperature upon excitation at 610 nm. Insert: Plot of I/I_0 versus the concentration of **C_{60}A** used to determine the binding constant $K_{A(P)}$ (4.0 x 10^4 M^{-1}). Please, compare with Figure S8.

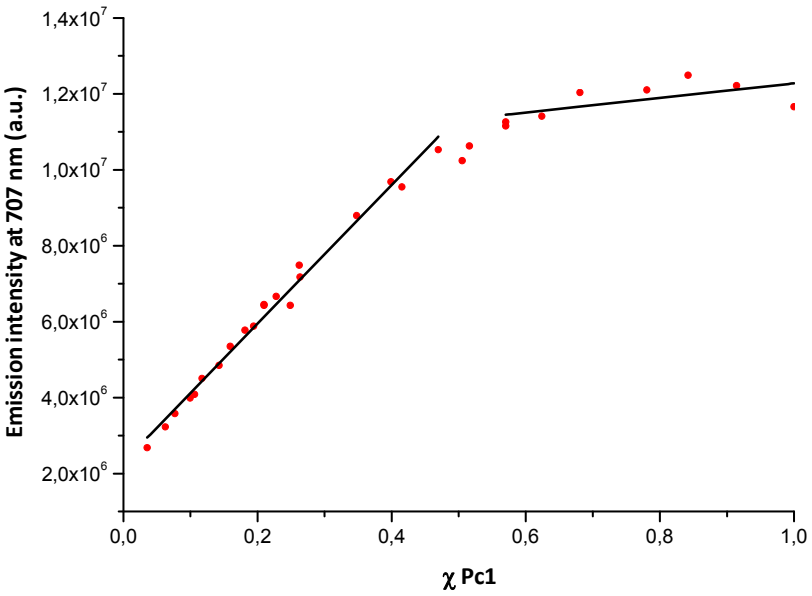

FIGURE S11. Job's plot obtained by mixing different relative concentration ratios of **Pc1** and **C_{60}A** in toluene solutions containing 1.50 x 10^{-5} M **DMAP** and recording the emission intensity at 707 nm. A slope change is observed at a molar fraction of 0.5, thus supporting the 1:1 **Pc1:C_{60}A** complex stoichiometry.

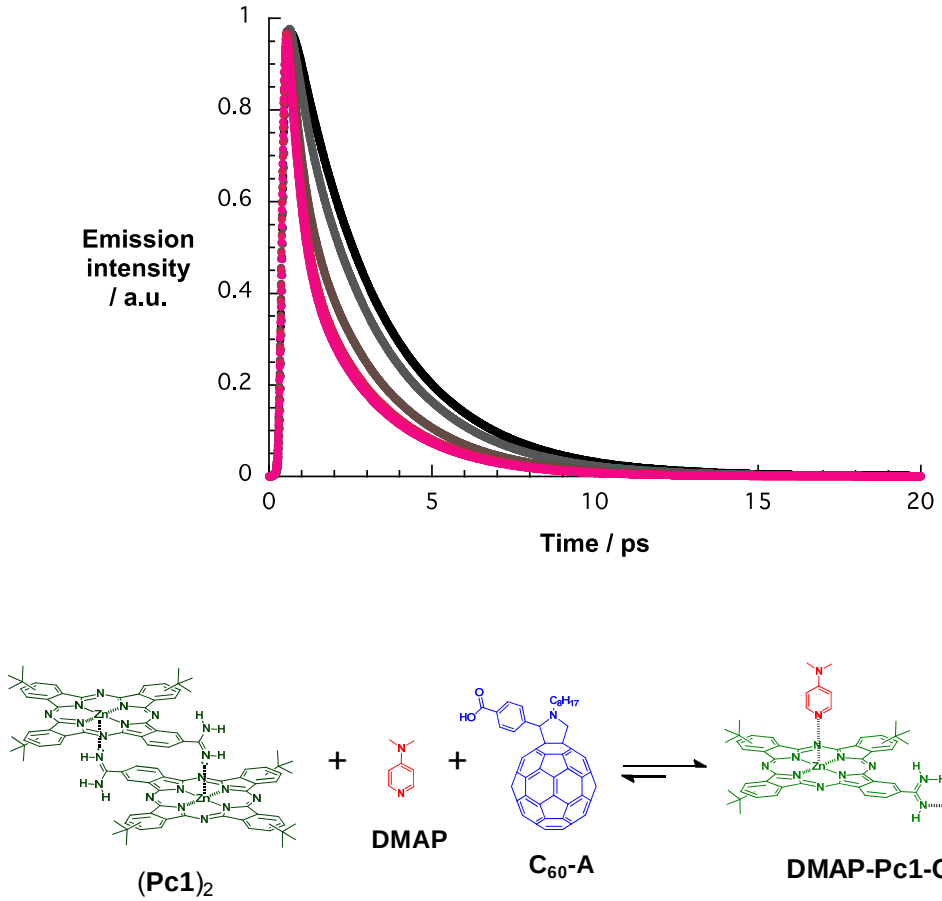

FIGURE S12. Fluorescence time profile obtained at different ratios of **DMAP-Pc1-C_{60}A** (0:1:0, 1:1:1, 2:1:2, 3:1:3 and 4:1:4, from black to red) in toluene at room temperature. The **Pc1** concentration was kept constant (1.43 x 10^{-5} M) and 647 was used as excitation wavelength and 700 nm as detection wavelength.

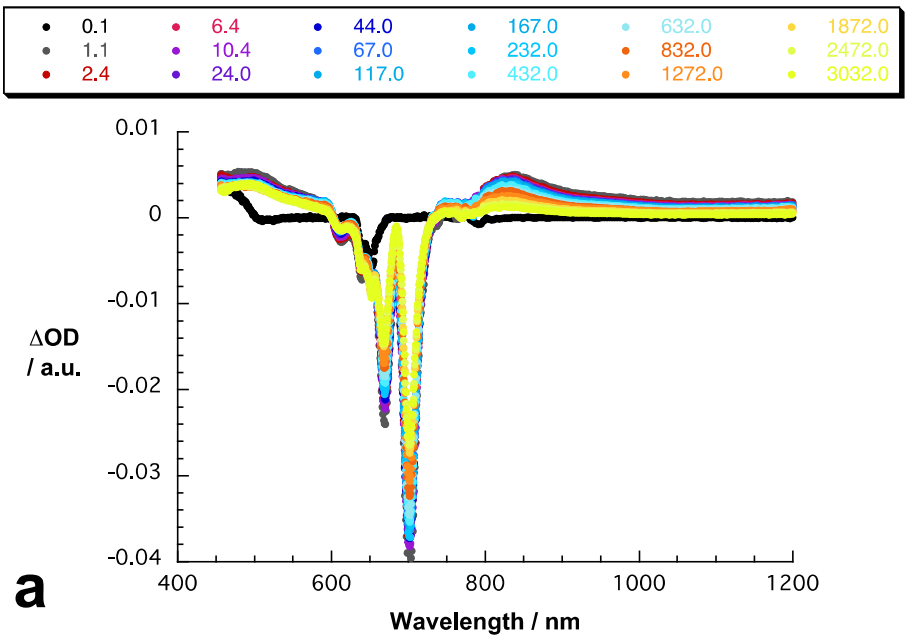
0.1
1.1
2.4
6.4
10.4
24.0
44.0
67.0
117.0
167.0
232.0
432.0
632.0
832.0
1272.0
1872.0
2472.0
3032.0
0.01
0
-0.01
-0.02
-0.03
-0.04
ΔOD
/ a.u.
400
600
800
1000
1200
Wavelength / nm
a

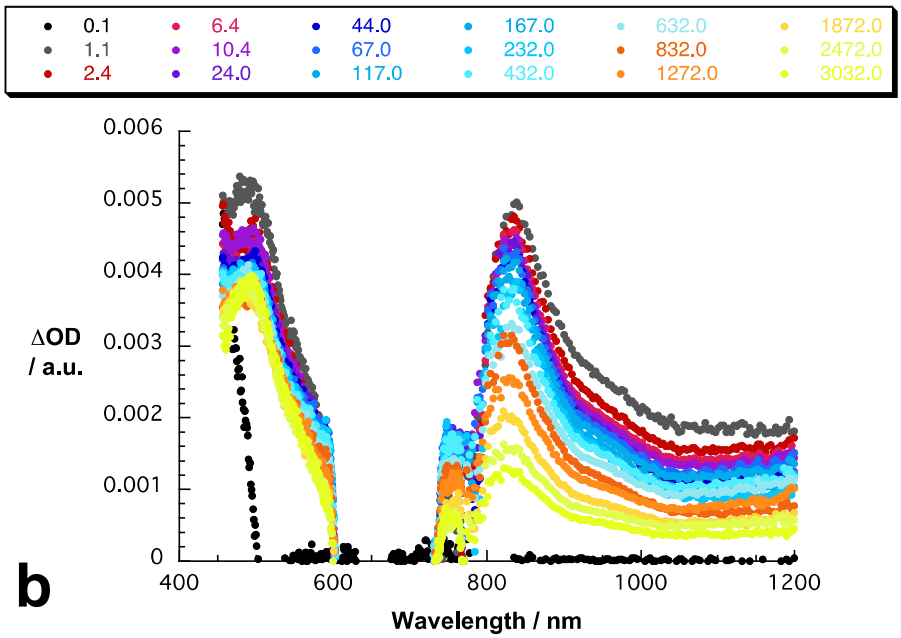
0.1
1.1
2.4
6.4
10.4
24.0
44.0
67.0
117.0
167.0
232.0
432.0
632.0
832.0
1272.0
1872.0
2472.0
3032.0
0.006
0.005
0.004
0.003
0.002
0.001
0
ΔOD
/ a.u.
400
600
800
1000
1200
Wavelength / nm
b

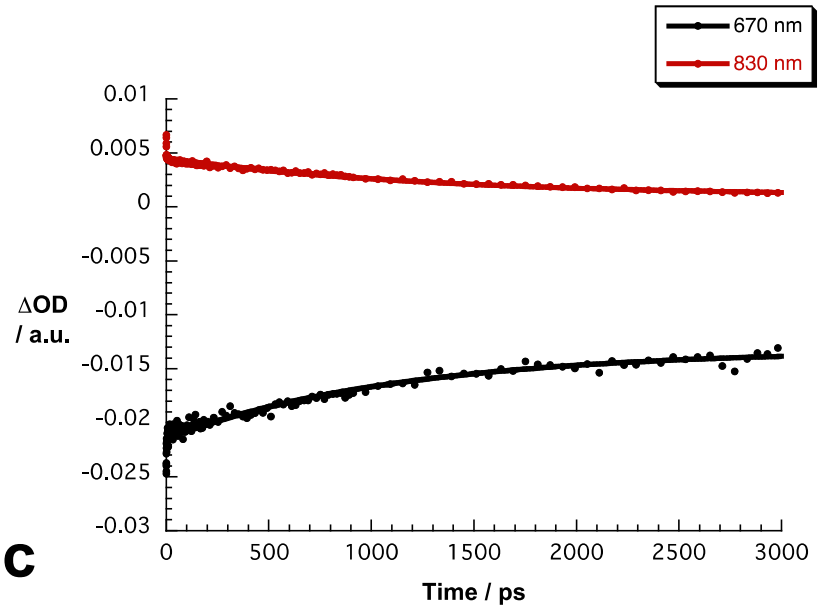

FIRGURE S13. (**a**) Differential absorption spectra (visible and NIR) obtained upon femtosecond flash photolysis (660 nm) of $(\mathbf{Pc1})_2$ in toluene with several time delays between 0.1 (black spectrum) and 3032.0 ps (yellow spectrum) at room temperature. (**b**) Zoom into differential absorption spectra (visible and NIR) obtained upon femtosecond flash photolysis (660 nm) of $(\mathbf{Pc1})_2$ in toluene with several time delays between 0.1 (black spectrum) and 3032.0 ps (yellow spectrum) at room temperature. (**c**) Time absorption profiles of the spectra shown above at 670 and 830 nm monitoring the triplet excited state decay.

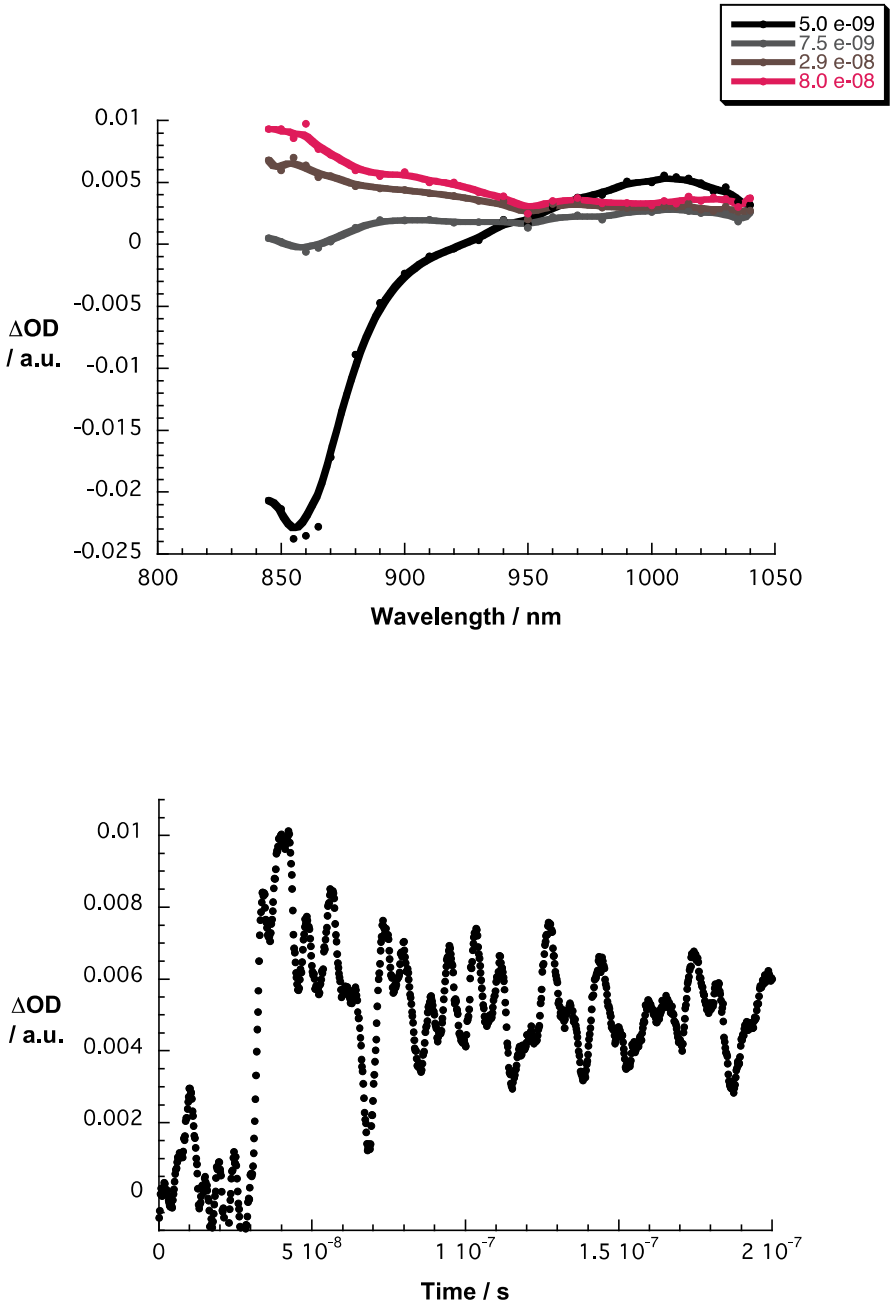

FIGURE S14. Upper part: differential absorption spectra (visible and NIR) obtained upon nanosecond flash photolysis (532 nm) of **DMAP-Pc1-C_{60}A** (4:1:4) in deaerated toluene with time delays of 5.0 x 10^{-9} s, 7.5 x 10^{-9} s, 2.9 x 10^{-9} s, and 8.0 x 10^{-8} s at room temperature. Lower part: Time absorption profile of the spectra shown above at 1010 nm (**C_{60}A** radical anion) monitoring the charge recombination.

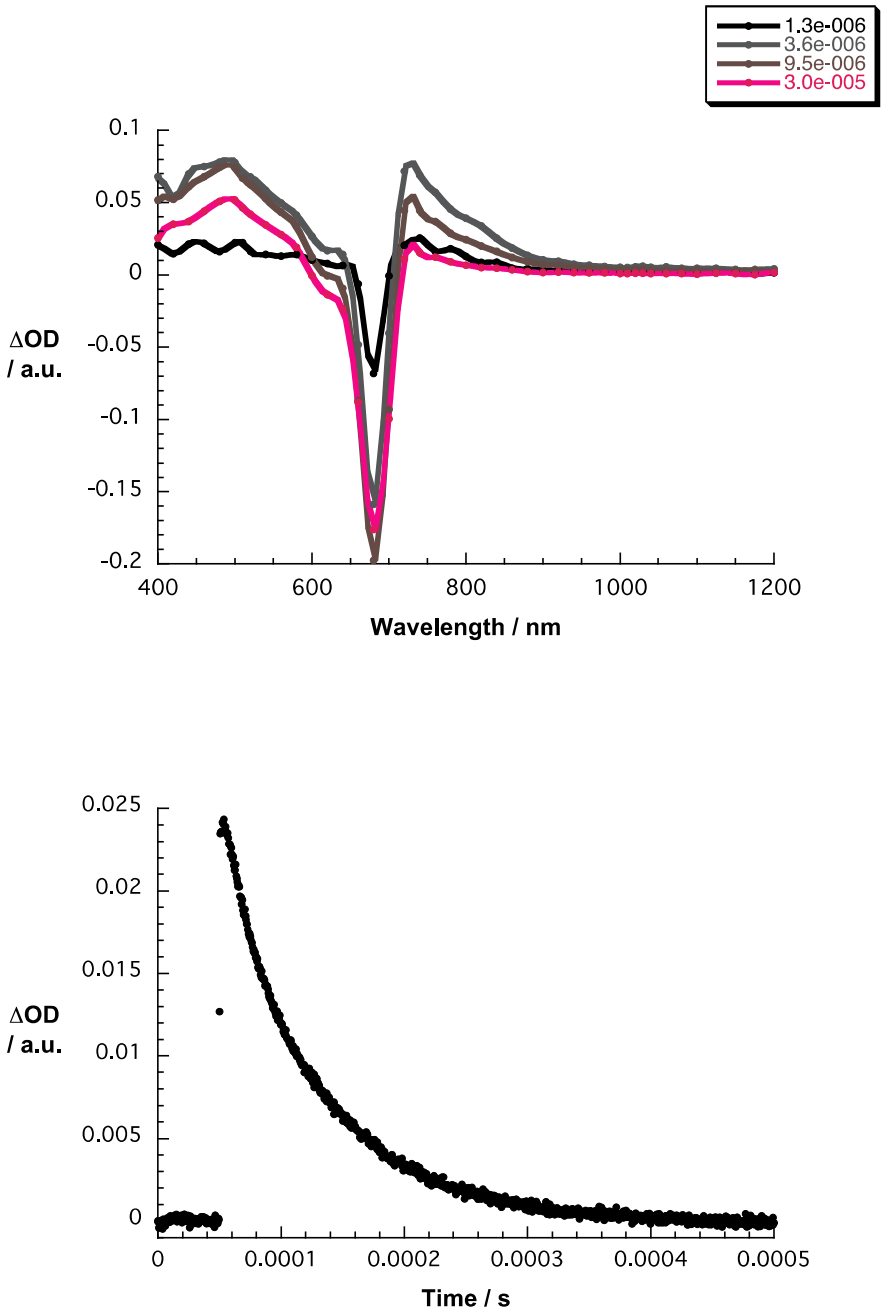

FIGURE S15. Upper part: Differential absorption spectra (visible and NIR) obtained upon nanosecond flash photolysis (532 nm) of **DMAP-Pc1-C_{60}A** (4:1:4) in deaerated toluene with time delays of 1.3 x 10^{-6} s, 3.6 x 10^{-6} s, 9.5 x 10^{-6} s and 3.0 x 10^{-5} s at room temperature. Lower part: Time absorption profile of the spectra shown above at 500 nm (**Pc1** triplet excited state) monitoring the triplet excited state decay.

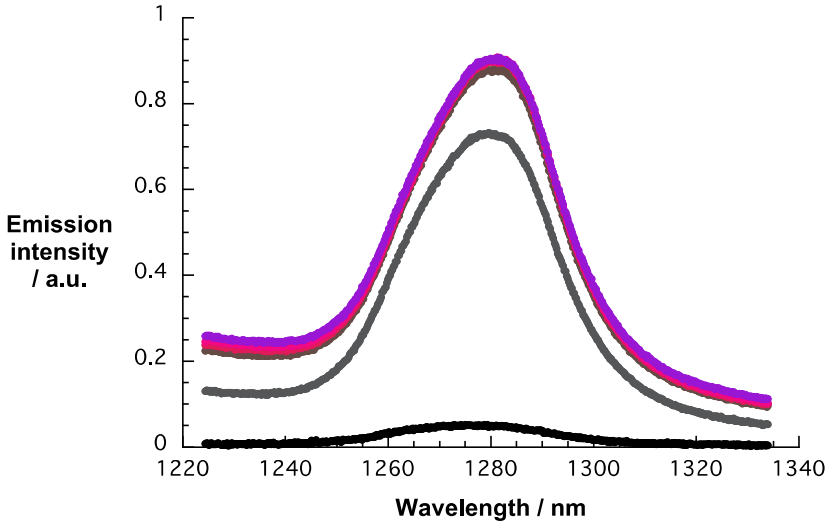

FIGURE S16. Singlet oxygen measurements obtained at different ratios of **DMAP-Pc1-C_{60}A** (4:0:4, 4:1:0, 4:1:1, 4:1:2, 4:1:3, and 4:1:4, from black to purple) in toluene at room temperature, showing the charge recombination into the triplet state of **Pc1**. The **Pc1** concentration was set to 1.2 x 10^{-5} M and 660 nm was used as excitation wavelength.

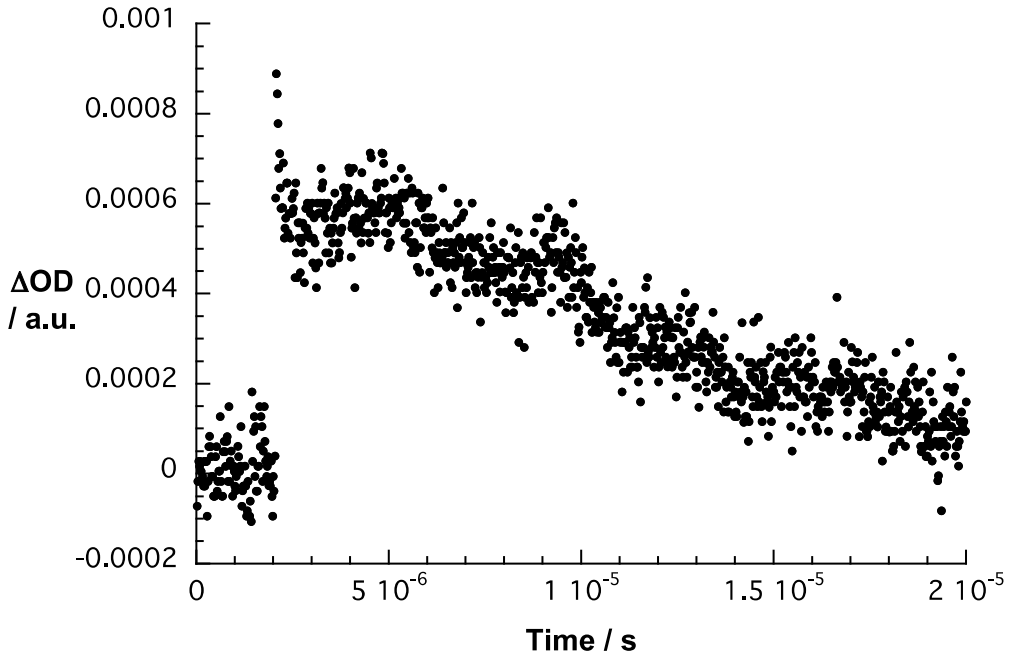

FIGURE S17. Time absorption profiles of the spectra shown in Figure 5 at 1015 nm monitoring the charge recombination.

References (S.I.)

[i] M. V. Martinez-Díaz, D. D. Díaz, *J. Porphyrins Phthalocyanines* **2009**, *13*, 369.

[ii] M. Segura, L. Sánchez, J. de Mendoza, N. Martín, D. M. Guldi, *J. Am. Chem. Soc*. **2003**, *125*, 15093.

[iii] V. Engelhardt, S. Kuhri, J. Fleischhauer, M. García-Iglesias, D. González-Rodríguez, G. Bottari, T. Torres, D. M.Guldi, R. Faust. *Chem. Sci.* **2013**, *4*, 3888–3893.

[iv] B. A. Anderson, E. C. Bell, F. O. Ginah, N. K. Harn, L. M. Pagh, J. P. Wepsiec, *J. Org. Chem.* **1998**, *63*, 8224.

[v] J. Otsuki, K. Iwasaki, Y. Nakano, M. Itou, Y. Araki, O. Ito, *Chem. Eur. J.* **2004**, *10*, 3461.

[vi] a) Y. Inaba, Y. Kobuke, *Tetrahedron* **2004**, *60*, 3097–3107; b) K. Kameyama, M. Morisue, A. Satake, Y. Kobuke, *Angew. Chem. Int. Ed.* **2005**, *44*, 4763-4766; c) A. Satake, O. Shoji, Y. Kobuke, *J. Organomet. Chem.* **2007***, 692*, 635–644.

[vii] M. García-Iglesias, PhD Thesis, Universidad Autonoma de Madrid, 2011.